Creep Behavior of a New Ni-base Single-crystal Superalloy, TMS-82+

Takehisa HINO, Yutaka KOIZUMI, Toshiharu KOBAYASHI, Shizuo NAKAZAWA, Hiroshi HARADA, National Research Institute for Metals,1-2-1 Sengen, Tsukuba Science City, Ibaraki 305-0047, Japan

Yomei YOSHIOKA, Toshiba Corporation Power & Industrial Systems Research & Development Center, 2-4 Suehiro-cho, Tsurumi-ku, Yokohama 230-0045, Japan.

The creep-strengthening mechanism of TMS-82+, which is a new Ni-base single-crystal superalloy developed at the National Research Institute for Metals in collaboration with the Toshiba Corporation, was investigated. The creep property of TMS-82+ is superior to that of other single-crystal superalloys, especially under high-temperature and low-stress conditions. As a result of a micro-structural observation of a creep-interrupted specimen, more continuous γ' platelets normal to the stress axis (a so-called raft structure) and a fine interfacial dislocation network are constructed in TMS-82+. These are considered to prevent the movement of dislocations and decrease the creep-strain rate.

1. INTRODUCTION

In contrast with steam turbine power plants, many combined cycle power plants have been operating successfully due to their high thermal efficiency and good operability.[1] A combined cycle power plant is mainly composed of gas turbines, steam turbines, and heat-recovery steam generators. The thermal efficiency of the combined cycle power plant can be improved by raising the inlet gas temperature of the gas turbines. To increase the inlet gas temperature, the materials for turbine blades and vanes are required to have higher creep-rupture strengths. Nibase single-crystal (SC) superalloys have higher creep strengths in comparison with conventionally cast and directionally solidified superalloys and are now used in the new-generation gas turbine plants. [2][3] It has been reported that the creep-rupture strengths of SC superalloys are improved by adding a Re element: second-generation SC superalloys contain about 3% Re, [4][5][6] and third-generation SC superalloys contain 5 to 6% Re. [6][7][8] However, it is also reported that adding Re to SC superalloys tends to cause Re-rich Topologically Closed Packed (TCP) phase precipitation, [10][11] which is known to reduce the creep-rupture strength. A new SC superalloy, TMS-82+, was developed by our group. [12] This alloy has superior creep properties and phase stability compared with second- and thirdgeneration SC superalloys, especially under high-temperature and low-stress conditions. In this paper, the creep-strengthening mechanism of TMS-82+ is investigated

2. MATERIALS AND METHODS

Table I shows the nominal composition of TMS-82+ and several second- and third-generation single crystal superalloys. Test specimens of TMS-82+ were cast into 10mm dia. bars using a directionally solidified furnace at the National Research Institute for Metals (NRIM). After checking that the longitudinal axes of these single-crystal bars were within 15° from the [001]

orientation, heat treatments were conducted using the following sequence.

· Solution heat treatment:

$$1280$$
°C / 1h \rightarrow 1300°C / 5h \rightarrow R.T. (A.C. or G.F.C)

· Aging heat treatment

1100°C / 4h
$$\rightarrow$$
 R.T.(A.C. or G.F.C)
 \rightarrow 870°C / 20h \rightarrow R.T.(A.C. or G.F.C)

After the heat treatments, creep test specimens (4mm dia. with 22mm gage section length) were machined from these singlecrystal bars. Creep tests were conducted between 900°C and 1100°C as well as 98MPa and 392MPa. In addition to this, to investigate the high-temperature creep mechanism, creepinterrupted tests were conducted under 1100°C/137MPa at 64 hours with TMS-82+ and TMS-75, at 4 and 260 hours with TMS-82+, and at 8 and 160 hours with TMS-75. TMS-75 is a third-generation SC superalloy also developed at NRIM.[7] Micro-structural examinations were conducted by transmission electron microscopy (TEM) and scanning electron microscopy (SEM). These specimens were cut into thin slices both normal and parallel to the longitudinal [001] directions. Thin foil specimens cut normal to the longitudinal [001] directions were used for TEM observation. These specimens were prepared using an electro-polishing method with a reagent consisting of 50 m ℓ HClO₄ and 250 m ℓ C₂H₄O₂ at 5°C. Specimens for SEM observation were mounted into molds, polished, and etched using a reagent consisting of 10 ml HNO3 and 30 ml HCl diluted by 40 mℓ C₃H₈O₃

Table I Chemical composition of tested and reference specimens

Alloy	Co	Cr	Мо	W	Al	Ti	Ta	Hf	Re	Ni
TMS-82+	7.8	4.9	1.9	8.7	5.3	0.5	6.0	0.1	2.4	Bal.
TMS-75	12.0	3.0	2.0	6.0	6.0	-	6.0	0.1	5.0	Bal.
Rene'N5	7.5	7.0	1.5	5.0	6.2	-	6.5	0.15	3.0	Bal.
CMSX-4	9.0	6.5	0.6	6.0	5.6	1.0	6.5	0.1	3.0	Bal.

3. RESULTS

Figure 1 shows the creep-rupture curves of TMS-82+, CMSX-4, [5] TMS-75, [8] Rene'N5, [7] Rene'N6, [6] MC653 [13], and a patent alloy (alloy 11) containing Ru. [14] The creep-rupture strength of TMS-82+ was superior to those of second-generation SC superalloys such as CMSX-4 and Rene'N5 in all stress and temperature ranges. The temperature capability of TMS-82+ at 137MPa/10⁵ hours was over 30°C higher than that of second-generation SC superalloys. Moreover, in the higher-temperature and lower-stress range, TMS-82+ was stronger than third-generation SC superalloys such as TMS-75 and Rene'N6 and even Ru-containing US-patented alloys. [14]

Figure 2 shows the creep curves of TMS-82+ and the third-generation SC superalloy TMS-75. Cross section micrographs of creep-interrupted specimens cut along the longitudinal direction on the middle of a specimen are shown in Figure 3. This figure shows the microstructures of TMS-82+ and TMS-75 at primary creep area, early stage of secondary creep area and end stage of secondary creep area, which is 70-80% of total creep life. A so-called raft structure is observed both in TMS-82+ and TMS-75; γ' precipitates are connected with each other normal to the stress axis in secondary creep areas. The raft structure is not constructed in the primary creep area in TMS-82+. However, once the raft structure is constructed, its morphology is more continuous than that of TMS-75 and is kept for a long time.

4.DISCUSSION

In this section, we discuss the effects of the raft structure on creep property. As mentioned above, a raft structure is observed both in TMS-82+ and TMS-75. Third-generation SC superalloys tend to precipitate the TCP phase, which is known to reduce the creep-rupture strength. [9][10] However, there are no precipitates of the TCP phase. The creep-strain rate of TMS-75 is, nevertheless, larger than that of TMS-82+, as shown in Table II. This suggests that the large creep-strain rate of TMS-75 in this condition does not result from the precipitation of the TCP phase. As for the morphology of the raft structure, more continuous γ' platelets are observed in TMS-82+ after 64 hours at 1100°C /137MPa compared with TMS-75. Moreover, the raft structure observed in TMS-82+ is kept longer than that of TMS-75. The raft structure improves the creep resistance by providing effective barriers to the dislocation climb around y' platelets.[15] Making a more continuous raft structure and keeping this structure for a long time are considered to disturb the dislocation motion effectively. This is considered to be the reason for the good creep property of TMS-82+. Table II also shows the lattice misfit of TMS-82+ and TMS-75 measured at 1100°C by X-ray diffraction techniques.^[16] The lattice misfit of TMS-82+ is negative, and the absolute value is larger than that of TMS-75. The large negative misfit enhances the y' rafting, [17] and TMS-82+ has a more continuous raft

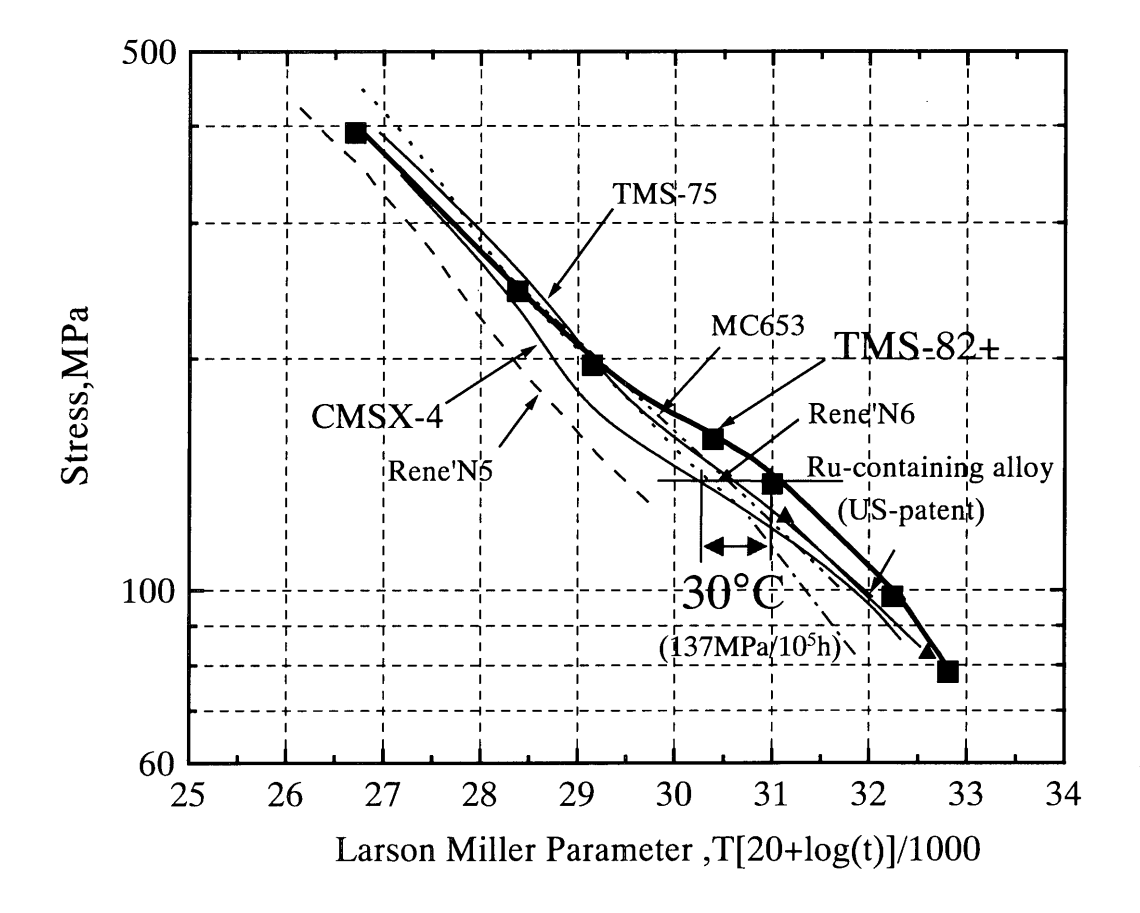


Figure 1 Creep-rupture strengths of TMS-82+, Rene'N5, CMSX-4, Rene'N6, TMS-75, MC653 and alloy11 (Ru-containg alloy) using the Larson Miller Parameter.

structure. Figure 4 shows TEM images of the interfacial dislocation network between the γ and γ' phases in the creep-interrupted specimens of TMS-82+ and TMS-75 after 64 hours at 1100°C/137MPa. The interfacial dislocation network is formed due to the misfit strain between the γ and γ' phases and additionally due to the applied stress of creep. From Table II, the amount of dislocation introduced by creep deformation in TMS-75 is seems to be larger than that of TMS-82+. On the other hand, the size of the dislocation network in TMS-82+ is finer than that of TMS-75. The dislocation induced by the creep is consider to be moved on the (111) plane and intersected with dislocation network formed on the (001) plane as illustrated schematically in Figure 5. It is considered that the relation between the dislocation

on the (111) plane and the (001) plane is similar to the relation between the dislocation and two obstacles. The force to bow the dislocation between two obstacles, τ , is expressed as the following equation.

$$\tau = \alpha Gb/R, \tag{1}$$

where α is a coefficient, G is a shear modulus, b is the Burgers vector, and R is the spacing between two obstacles. As for the force between the dislocation induced by creep and the interfacial dislocation network, R is the radius of the dislocation network spacing. From this equation, a large force is necessary to bow a dislocation to radius R in the fine dislocation network.

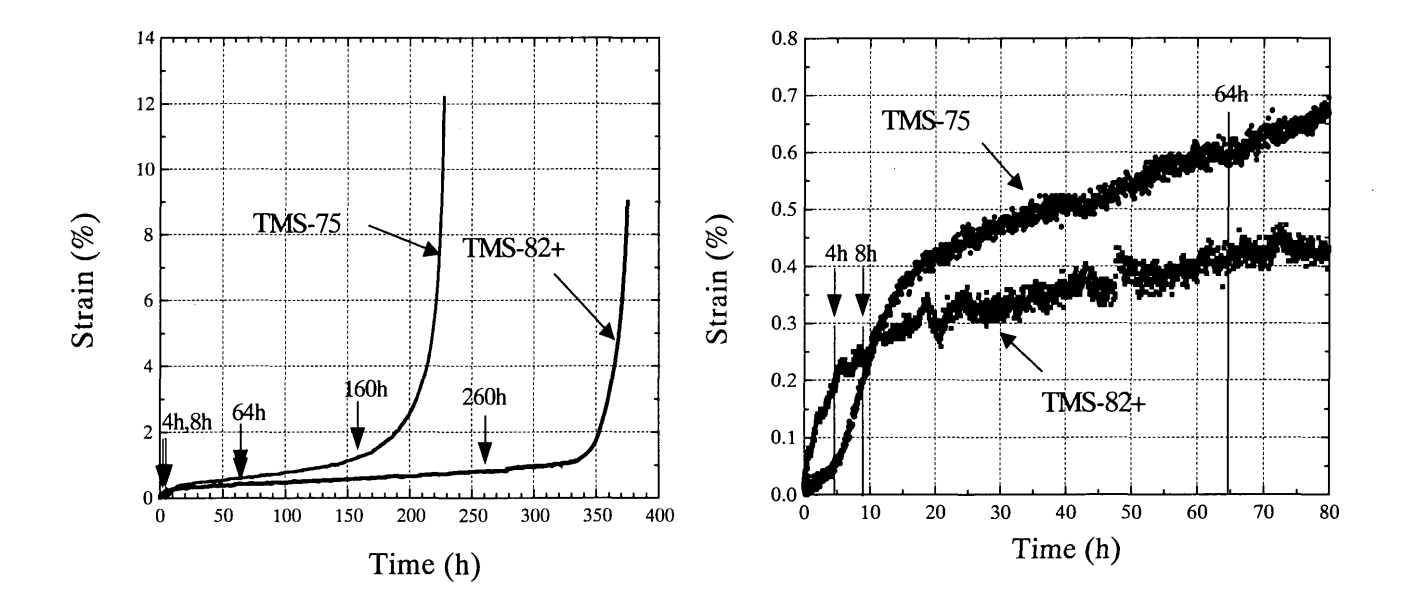


Figure 2 Creep curves of TMS-82+ and TMS-75 under a 1100° C/137MPa condition.

	Primary Creep Area	Early Stage of Secondary Creep Area	End Stage of Secondary Creep Area		
TMS-82+	4h	64h	260h		
TMS-75	8h	64h	/160h		

Figure 3 Raft structures in TMS-82+ and TMS-75; creep interrupted at (a) primary creep area, (b) early stage of secondary creep area and (c) end stage of secondary creep area under a 1100°C/137MPa condition.

Table II Lattice misfit, creep strain, and creep-strain rate of TMS-82+ and TMS-75 at 64 hours of creep under 1100°C/137MPa.

Alloy	Lattice misfit (1100°C)	Creep strain	Creep-strain rate	
TMS-82+	-0.24	0.409%	2.4×10 ⁻³ %/h	
TMS-75	-0.17	0.593%	3.4×10 ⁻³ %/h	

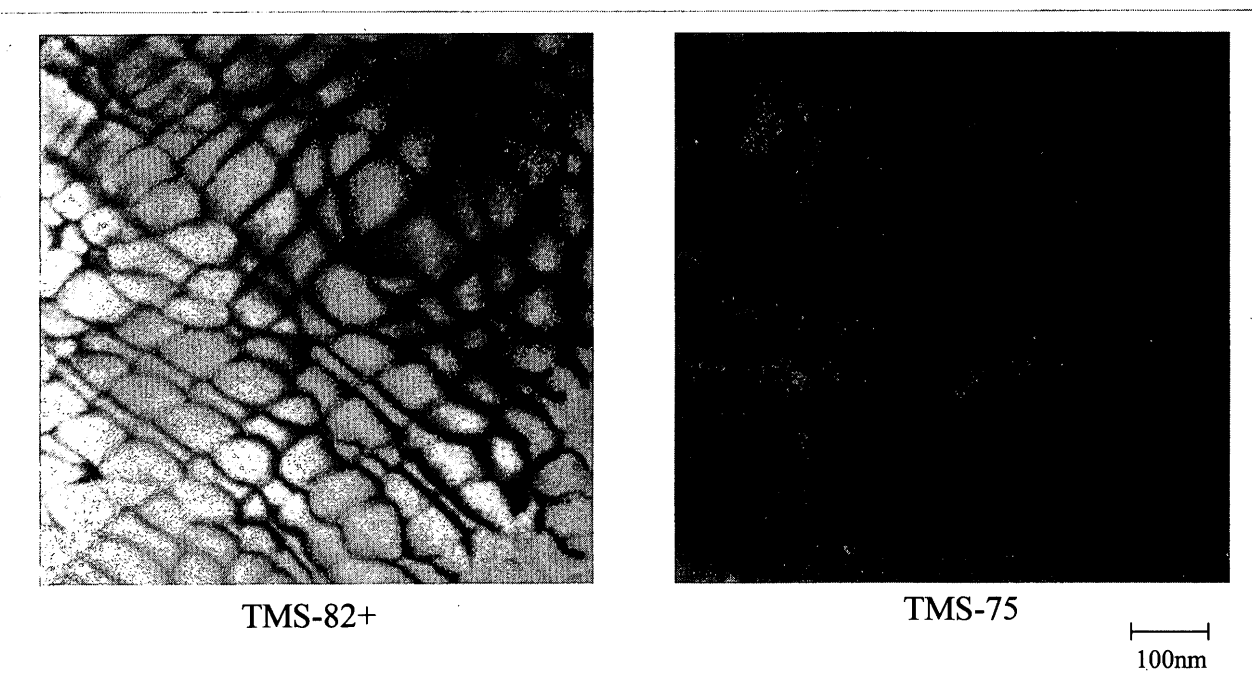


Figure 4 Dislocation network on the γ/γ'interface in (a)TMS-82+ and (b)TMS-75; creep interrupted at 64 hours under a 1100°C/137MPa condition; foil prepared perpendicular to the stress axis.

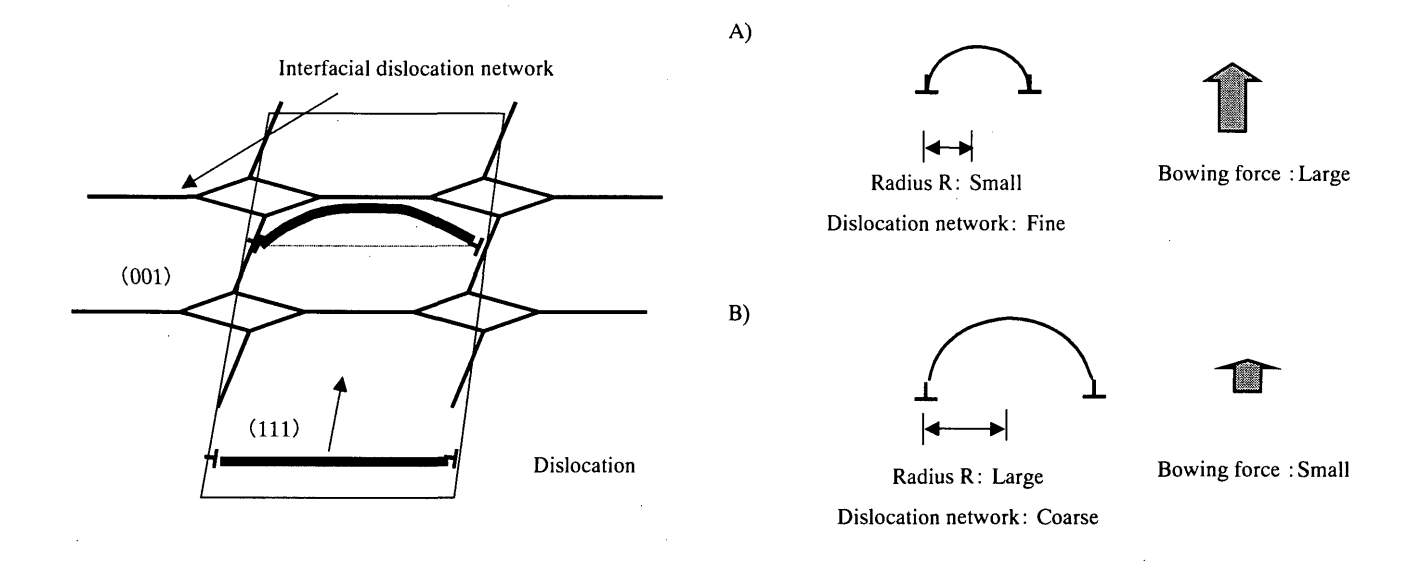


Figure 5 Schematic illustration of the interaction between the interfacial dislocations network and dislocations induced by creep.

This is another reason that TMS-82+ has high creep-rupture strength compared with other second- and third-generation SC superalloys. Once a good rafted structure is established, as in TMS-82+, dislocation climbing is considered to be became very difficult. Under this condition, dislocation cutting into the γ' platelet is forced to be the predominant creep mechanism, and then, a finer dislocation network can act as a very effective barrier to this. As a result, the creep property of TMS-82+ is superior to that of other SC superalloys under high-temperature and low-stress conditions.

5. CONCLUSIONS

In this study, the creep-strengthening mechanism of TMS-82+ was investigated. The following results were obtained.

- In the micro-structural observation, the length of the raft structure normal to the stress axis of TMS-82+ is longer than that of the third-generation SC superalloy, TMS-75. The raft structure constructed in TMS-82+ is kept for a long time, which is a reason for the superior creep property of TMS-82+ compared to that of other SC superalloys under high-temperature and low-stress conditions.
- 2. The size of the dislocation network of TMS-82+ is finer than that of TMS-75. This is considered to be another reason that the creep property of TMS-82+ is superior to that of other SC superalloys.
- TMS-82+ has a large negative lattice misfit between γ and γ' phases that accelerates the formation of the more continuous raft structure and a very fine dislocation network.

6.ACKNOWLEDGEMENTS

This work has been carried out within a research activity of High Temperature Materials 21 Project. We would like to express our sincere thanks to Dr. M. Maldini (Now at CNR-TEMPE, Italy), Mr. T. Yokokawa, Dr. H. Murakami, Dr. Y. Yamabe-Mitarai, Mr. S. Nakazawa, Dr. M. Osawa, and Mr. M. Sato of the National Research Institute for Metals for their advice. We would

like to express our sincere thanks to Dr. P.E. Waudby of Ross & Catherall Ltd. for making the master ingot and analyzing the composition of alloys.

REFERENCES

- [1]T.Aizawa, Proc.of 1995 Yokohama int. gas turbine congress, No3(1995), p.341- 348.
- [2]H.Yokoyama, 28th gas turbine seminar text, (in Japanese),(2000),p.77-86.
- [3]I.Myougan, 28th gas turbine seminar text, (in Japanese),(2000), p.101-110.
- [4]A.D.Cetel and D.N.Duhl, Proc. of 6th International Symposium on Superalloys, (1988), p.235-244.
- [5]G.L.Erickson and K.Harris, Proc. of Material for Advanced Power Engineering 1994, Part I, (1994), p. 1055-1074.
- [6] W.S. Walston et.al., Proc. of 8th International Symposium on Superalloys, (1996), p.27-34.
- [7]G.L.Erickson, Proc. of 8th International Symposium on Superalloys, (1996), p.35-44.
- [8]Y.Koizumi et.al., Proc. of Material for Advanced Power Engineering, Part II, (1998), p.1089-1098.
- [9]R.Darolia et.al., Proc. of 6th International Symposium on Superalloys, (1988), p.255-264.
- [10]T.Hino et.al., Proc. of Material for Advanced Power Engineering, PartII, (1998),p.1129-1137.
- [11]T.Yamagata et.al., Proc. of 5th International Symposium on Superalloys, (1984), p.157-166.
- [12]T.Hino et.al., Proc. of 9th International Symposium on
- Superalloys, (2000),p. 729-736 [13]P.Caron, Proc. of 9th International Symposium on
- Superalloys, (2000), p.737-746
 [14]K.S.O'hara et.al., U.S.Patent 5,482,789 "Nickel Base Superalloy and Article".
- [15] Rebecca A. et.al, Proc. of 5th International Symposium on Superalloys, (1984), p.135-144.
- [16]T.Yokokawa and M.Osawa, private communication with author, National Research Institute for Metals, 25 Februrary
- [17]D.D.Pearson et.al., Proc. of 4th International Symposium on Superalloys, (1980) ,p.513-520